Ring-Shaped Vortex Domain in Type-II Superconductors

A. Gröger,[1,*] A. Böhm,[1] U. Beyer,[1] B. Ya. Shapiro,[2] I. Shapiro,[2] and P. Wyder[1]

[1]*Grenoble High Magnetic Field Laboratory, Max-Planck-Insitut für Festkörperforschung and Centre National de la Recherche Scientifique, 25, rue des Martyrs, F-38042 Grenoble Cedex 9, France*

[2]*Institute of Superconductivity, Bar-Ilan University, 57100 Ramat-Gan, Israel*

(Received 21 August 2002; revised manuscript received 3 March 2003; published 11 June 2003)

We present results of experiments in superconducting niobium and numerical simulations showing the creation of a metastable ring-shaped vortex domain by heating. Such vortex rings, if pinned by structural defects, can exist forever.

DOI: 10.1103/PhysRevLett.90.237004 PACS numbers: 74.25.Op, 74.25.Qt

Symmetry-breaking phase transitions are an important subject of research in many areas of physics from condensed matter in thermodynamical equilibrium to nonequilibrium systems undergoing quench [1]. With reference to cosmological models, Kibble [2] stressed that topological defects have played a fundamental role in the evolution of the early Universe. Zurek captured the general feature of the rapid cooling pointing out the similarity between the cosmological phase transition and some specific experimental phenomena in solid state physics, in particular, in liquid helium ^{3}He [1], where vortices emerge in the rotating cylinder, while superfluidity in the center of cylinder has been previously destroyed by the heat impact. In this case, the usual Kibble-Zurek scenario, initially developed for homogeneous systems, has been modified for spatially inhomogeneous quench [3].

Superconductors, being well understood and experimentally accessible systems, can serve as a probe for studying string formation. Vortices and antivortices here play the role of topological defects in the Kibble-Zurek scenario. In addition, probing superconductors allows one to extend the Kibble-Zurek mechanism to a system with local gauge symmetry (in contrast to ^{4}He ^{3}He systems, which have a global gauge) (see [4]).

In the present publication, we investigate experimentally the recovery of superconductivity and the vortex generation in the case which is very similar to that of liquid ^{3}He. In particular, we study the recovery of superconductivity in niobium subjected to an external magnetic field after the superconductivity has been locally destroyed by heating. We have measured the spatial distribution of normal and superconducting domains after the recovery of the superconductivity and compare the results to numerical simulations based on the set of Ginzburg-Landau equations, coupled with the thermal diffusion equation. We have found a ring-shaped normal conducting domain predicted by theory [5] which we associate with a cluster of pinned Abrikosov vortices. This structure is different from the usual hexagonal vortex lattice growing in thermal equilibrium.

The basic outline of the experiment is shown in Fig. 1. By projecting light of an Ar-Ion-laser on one side of the sample, a heated zone (''hot spot'') is created. The light is modulated at a frequency of about 100 Hz by an optical chopper and it is coupled into an optical fiber by means of microscope optics. The fiber is positioned about $20 \ldots 50$ μm from the sample surface and can be moved by a mechanical micropositioning device [6]. The modulated light leaving the fiber heats the sample surface periodically in the hot spot that has a diameter of about 5 μm. Heat conduction in the sample leads to a diameter of the effectively heated zone of about 20 μm. The laser power at the sample surface is about 25 mW. A magnetic field B can be applied perpendicularly to the sample surface keeping the sample in the mixed state with B between the two critical magnetic fields. The whole

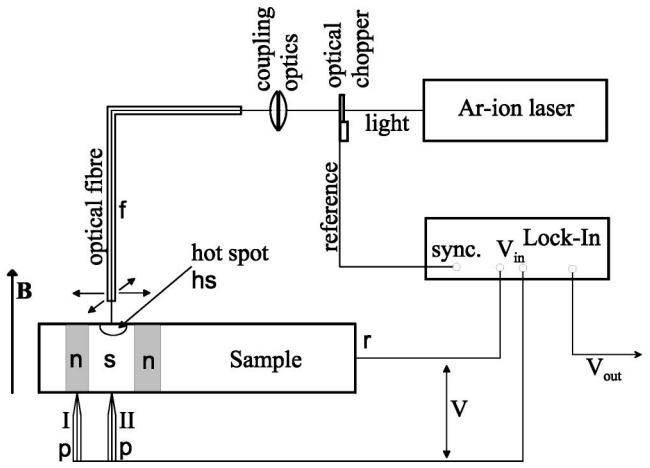

FIG. 1. Principle of the experiment: laser light creates a normal conducting hot spot *hs*. The current induced by the periodic heating causes a voltage drop between the detecting point contact *pc* and the reference contact *r* when it passes a normal conducting domain *n*. When passing a superconducting domain *s*, no voltage drop occurs. Thus, in position 1 a signal V is measured and in position 2, V will be zero. In the experiment, the optical fiber *f* is moved to obtain spatial resolution while the point contact *p* is kept in a fixed position.

 © 2003 The American Physical Society

setup is immersed in liquid ^{4}He at a temperature of 4.2 K.

The samples were first cut by spark erosion from single crystals to slabs of ≈ 2 mm thickness. This thickness was further reduced by chemical etching to 0.15(edges) . . . 0.3(middle) mm. Thus, the undisturbed bulk is exposed and the thickness is in the order of magnitude of the mean free path at liquid ^{4}He temperatures. The residual resistance ratio of 2500 assures a relatively long mean free path of the electrons and sufficient structural defects serving as pinning centers.

In order to distinguish the superconducting phase (s) from the normal conducting phase (n) in the vortex cores, we measure the voltage between a point contact (p) on one surface of the sample and a reference contact (r) on the edge of the sample while the hot spot (hs) is periodically heated and cooled by the laser light and the helium bath, respectively.

If the sample material at the contact position is in the normal conducting state (position I), the sample has a finite resistance giving rise to a voltage drop. On the contrary, if the contact is in a position where the sample is superconducting (position II), there will be no voltage drop and the measured signal V will be zero. We are thus able to discriminate normal and superconducting phases in the sample by observing the voltage drop. The voltage drop is created by a current generated entirely by the temperature gradient, no externally generated current is applied. It should be noted that the normal conducting domains consist of individual vortices and the sample is superconducting between the vortices. Thus, the voltage drop occurs only when there is a vortex at the detection contact position. If there is no vortex at the detection contact position, the current between the detection and the reference contact can pass in between the vortices as an entire supercurrent. Typical contact resistances were in the order of 1 Ω. The measured potentials V for the data shown in Fig. 2 range from -220 to -115 nV. The background voltage is most probably due to a contact voltage between the detection point contact and the sample, as suggested by our experience with the experimental technique and the apparatus.

Figure 2 shows the spatial voltage distribution measured in an external magnetic field of 0.1 T. We see a ring-shaped voltage distribution with a sharp peak approximately in its center. The large ring has a mean diameter of 600 μm and a ring width of about 250 μm. As explained, we associate the regions in which we observe a voltage drop with the normal conducting regions.

The recovery of superconductivity in the hot spot after switching off the heating has been simulated numerically by solving the set of time-dependent three-dimensional Ginzburg-Landau (TDGL) equations coupled with the equation of thermal diffusion.

The initial condition has been chosen to be a normal domain with radius R penetrating the entire sample thickness surrounded by the superconductor. Where the temperature exceeded the critical value, the order parameter ψ was suppressed ($\psi = 0$). A total magnetic flux Q was assumed to be trapped in the normal domain.

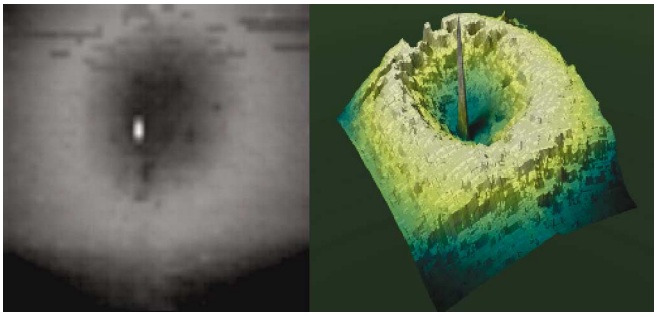

FIG. 2 (color). Imaging of ring-shaped vortex domains in Nb: Left: gray scale representation of the signal V as a function of xy real space coordinates on the sample surface. The applied magnetic field is $B = 0.1$ T perpendicular to the image plane. Image frame: 800×800 μm, 60×60 measured points. The gray scale ranges from -220 nV (black) to -115 nV (white) measured between the point and reference contacts. A normal conducting vortex ring appears around a sharp peak. The sharp peak is due to the normal conducting heated region (''hot spot''). Right: perspective representation of the same data.

A typical scenario of the evolution described by the TDGL equations is as follows [5]. When the sample is locally heated, a macroscopic normal conducting region (hot spot) attracts Abrikosov vortices from the outside to enter the hot spot. Even if the initial heating did not create a normal domain extending over the entire sample thickness, the incoming vortices will destroy the superconductivity below the hot spot and create a normal domain that extends over the entire sample thickness. The magnetic flux entering the hot spot increases its topological charge. Directly after the heating has stopped, the recovery of superconductivity in the normal domain containing magnetic flux starts when the temperature front where $T = T_c$ loses its contact with the front of the order parameter. The temperature front velocity V_T always increases with time while the order parameter front, pressing the magnetic flux, confined inside the hot spot is slowing down and its velocity v_F decreases towards zero. The normal domain ($T < T_c$ and $\psi = 0$) appearing between these two fronts is apparently unstable with respect to the creation of Abrikosov vortices. On the other hand, this instability can be suppressed by the moving front of the order parameter ''washing out'' the growing vortices. The fully developed vortices arise when the characteristic time of vortex growth t_Z (here $t_Z \sim \sqrt{t_0/\gamma}$ is a Zurek's characteristic time) is less than the characteristic sweep time $t_S \sim L(t)/v_F$, which is the time when the front of the order parameter sweeps the normal unstable domain between the two fronts, the size of which is $L(t)$.

$$L(t) = \int_{t_0}^{t} (V_T - v_F)dt. \quad (1)$$

In contrast to the $1D$ case described by Kopnin and Thuneberg [3], where the order parameter and temperature fronts move with the same velocity, in our geometry the full-size vortices always have to emerge because of the permanently decreasing magnitude of the order parameter front velocity and the essential acceleration of the temperature front. Depending on the cooling regime, various vortex configurations appear. If the size of the normal unstable domain is of the order of 10ξ with ξ being the correlation length and the sweep time t_S slightly exceeds the characteristic time of vortex growth t_G then only part of the topological charge confined inside the hot spot is released resulting in the ring of Abrikosov vortices (Fig. 3), while the rest remains in the central spot area where the temperature still exceeds the critical one. The front of the order parameter accelerates after the shrinking hot spot looses its topological charge. In this moment, voltage produced by the moving flux front increases significantly.

Such released vortex rings move with decreasing velocity until they are finally trapped by defects of the crystal acting as pinning centers while the remaining normal domain is shrinking continuously further. The front of the order parameter accelerates after that and the above-mentioned dynamics might repeat itself. In this case, a new vortex ring emerges forming a ring-shaped cluster. The ring structure is immobilized by the pinning centers and could in principle remain forever. If the hot spot is quenched quickly, then the Abrikosov vortex lattice may grow across the entire unstable domain [5].

It should be noted that the vortex structure emerging from the cooling normal domain depends crucially on the sample's properties. In particular, a significant increase of the parameter $\chi = 4\pi\sigma D/c^2$ (where D is the thermal diffusion coefficient and σ is the conductivity) from 2×10^{-2} to 5×10^{-1} results in transformation of the emerging vortex structure from concentric vortex rings to a regular Abrikosov vortex lattice.

Now comparing Figs. 2 with those from Ref. [5], we see both in experiment and numerical simulation a normal conducting ring structure emerging from the relaxing normal state. Applying the presented model, we explain the experimentally observed normal conducting ring structure by the normal conductivity of the vortex cores emerging from the relaxing hot spot. The outgoing propagating vortices produce a voltage proportional to their velocity and the topological charge. An electric voltage peak is expected to be registered when vortices cross the normal conducting detection point contact. Thus in the case of only one heating/cooling cycle and a detecting resolution in the 10 μm range a sharp ring structure may be detected. On the other hand, the decreasing vortex hydrodynamics velocity and the statistically distributed pinning centers may result in a pinning of the vortex ring at a statistically determined distance. We obtain in the experiment a broadened voltage distribution in real space probably due to two factors: the experimental resolution of several tens of micrometers implies a spatial averaging over several vortices. Moreover every measured point in the experiment represents an averaging over many heating and cooling cycles. So during every measurement cycle many vortex rings are generated and pinned at different positions with a statistical distribution, giving rise to an additional broadening of our signal in real space. The obvious difference between the diameters of the ring structures in simulation and experiment can be explained by the time scales involved. While the numerical results presented in Ref. [5] cover only an initial process of the vortex ring creation when the time range

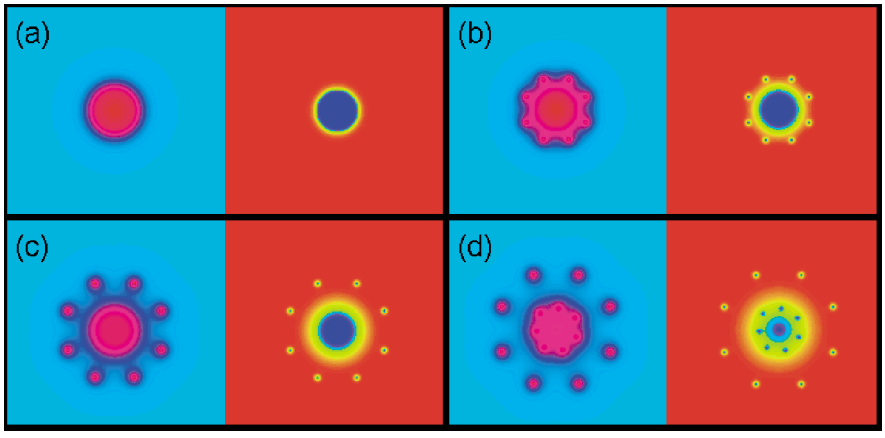

FIG. 3 (color). Numerical simulation of vortex ring creation: in each panel (a) to (d), the left side (blue background) shows the temperature distribution, whereas the right side (red background) shows the distribution of the order parameter (red: 1, blue: 0). The initial topological charge was 16 and the radius of the hot spot 4×10^{-5} cm, the diffusion coefficient was 0.009 cm^2/s. Time evolution at (a) $t = 0$, (b) $t = 2 \times 10^{-9}$ s, (c) $t = 1.2 \times 10^{-8}$ s, (d) $t = 5 \times 10^{-7}$ s.

of 5×10^{-7} s, that is still almost immediately after the starting of cooling, the time scale of the experiments is 0.1 s. During this time, the vortices emerge to form a ring structure of a diameter that is significantly larger than the diameter of the initial hot spot. Taking into account numerical estimations that vortices move with mean velocity $V_v \sim 10^{-1}$ cm/s [7] we obtain that for the experiment time scale 0.1 s vortices form ring with radius $R \sim 10^{-2}$ cm, which is in a good agreement with the experiment. The crucial question adressed by this Letter is the origin of the observed vortex configuration that is different from the usual Abrikosov lattice. Such an explanation is provided by the scenario that we described.

The scenario discussed here theoretically and experimentally is a rather general one. In principle, it should be true for any broken symmetry phase transition as, for example, crystallization of solids, appearance of smectic structure in liquid crystals, and maybe even for some cosmological models describing cosmic string formation.

From the above, we conclude that we have observed ring structures consisting of superconducting vortices. These are formed by creating vortex rings by explosive nucleation when the superconductivity is recovered after being destroyed by heating as described in the theory by Shapiro *et al.* [5]. The vortex rings emerge from the shrinking hot spot until they are finally pinned and thus form a metastable configuration that is different from the Abrikosov vortex lattice that is formed in thermal equilibrium.

We would like to thank J. Heil who developed the scanning apparatus and spent many hours in introducing us to its usage, P. Keppler and J. Major for growing the niobium single crystal as well as E. Polturak, P.Esquinazi, and V. Kogan for interesting and helpful discussions. One of the authors (B. Ya. S.) specially thanks the Binational Israel-USA Foundation, Binational Israel-Germany Foundation, and the Minerva Centre at Bar-Ilan for permanent support.

*Present address: Universität Würzburg, Physikalisches Institut (EPIII), Am Hubland, D-97074 Würzburg, Germany.

[1] W. H. Zurek, Phys. Rep. **276**, 177 (1996).
[2] T. M. Kibble, J. Phys. A **9**, 1387 (1976).
[3] N. B. Kopnin and E. V. Thuneberg, Phys. Rev. Lett. **83**, 116 (1999); I. S. Aranson, N. B. Kopnin, and V. M. Vinokur, Phys. Rev. Lett. **83**, 2600 (1999); G. E. Volovik, Physica (Amsterdam) **280B**, 122 (2000).
[4] M. Hindmarsh and A. Rajantie, Phys. Rev. Lett., **85**, 4660 (2000).
[5] I. Shapiro, E. Pechenik, and B. Ya. Shapiro, Phys. Rev. B **63**, 184520 (2001).
[6] J. Heil, A. Böhm, A. Gröger, M. Primke, P. Wyder, P. Keppler, P. Major, H. Bender, E. Schönherr, H. Wendel, B. Wolf, K. U. Würz, W. Grill, H. Herrnberger, S. Knauth, and J. Lenzner, Phys. Rep. **323**, 387 (2000); J. Heil, A. Böhm, M. Primke, and P. Wyder, Rev. Sci. Instrum. **67**, 307 (1996).
[7] D. Saint-James, G. Sarma, and E. J. Thomas, *Type II Superconductivity* (Pergamon Press, Oxford, 1969), p. 233.